Inorg. Chem. **2004**, *43*, 1302–1310

An Expanded Set of Functional Groups in Bis(dithiolene)tungsten(IV,VI) Complexes Related to the Active Sites of Tungstoenzymes, Including W^{IV}–SR and W^{VI}–O(SR)

Jianfeng Jiang and R. H. Holm*

Department of Chemistry and Chemical Biology, Harvard University, Cambridge, Massachusetts 02138

Received October 24, 2003

The active sites of tungstoenzymes have the formulations $W^{IV,V}L(S_2pd)_2$ and $W^{VI}LL'(S_2pd)_2$, in which two pyranopterindithiolene cofactor ligands (S_2pd) are chelated to a tungsten atom. Ligands L and/or L′ are not fully defined in any wild-type enzyme. The feasibility of various coordination fragments (functional groups) in potential bis(dithiolene)tungsten site analogues has been examined in previous work by exploratory synthesis. This investigation expands the range of accessible functional groups. The synthetic scheme originates with $[W(CO)_2(S_2C_2Me_2)_2]$, whose carbonyl groups are labile to substitution. Complexes $[W^{IV,VI}LL'(S_2C_2Me_2)_2]^{1-}$ are described in terms of their functional groups $W^{IV,VI}LL'$. Reaction of the dicarbonyl with formate in acetonitrile/THF affords $W^{IV}(CO)(\eta^1\text{-}HCO_2)$ (**4**) and in Me_2SO $W^{VI}O(\eta^1\text{-}HCO_2)$ (**7**) by an oxo transfer reaction. Carboxylates yield six-coordinate $W^{IV}(\eta^2\text{-}O_2CR)$ (**1**–**3**, R = Ph, Me, Bu^t) with C_{2v} symmetry. Reaction of **3** (R = Bu^t) with Me_3SiSR (R = C_6H_2-2,4,6-Pr^i_3) gives $W^{IV}(SR)$ (**5**), which undergoes oxo and sulfido atom transfer to form $W^{VI}O(SR)$ (**8**) and $W^{VI}S(SR)$ (**9**), respectively. Attempts to prepare corresponding selenolate complexes, pertinent to the active site of formate dehydrogenase, were unsuccessful, including reactions of $W^{VI}OCl$ (**10**) with RSe^-. Structure proofs of **2**–**10** were obtained by X-ray structure determinations. Some 26 functional group types in bis(dithiolene)W(IV,V,VI) molecules have now been achieved by synthesis. It remains to be seen which are incorporated in an enzyme site. A number of them (e.g., **5**) are directly analogous to molybdoenzyme sites, and may possess corresponding reactivity with biological substrates, as do $W^{IV}(OR)/W^{VI}O(OR)$ (prepared earlier) in the reduction of *N*- and *S*-oxides by atom transfer.

Introduction

The discovery and characterization of tungsten-containing enzymes[1−5] provides an unanticipated opportunity for the development of synthetic systems that can potentially disclose intrinsic structural and reactivity aspects of active sites. These enzymes derive from bacterial or archaeal sources and have been classified into two major groups, the AOR and F(M)DH families.[1,2,6] While these enzymes as a class are undergoing continuing delineation, the *complete* active site structure of any wild-type enzyme in any physiological oxidation state ($W^{VI,V,IV}$) remains undefined. The most significant structural feature is the presence of *two* pyranopterindithiolene cofactor ligands bound in the oxidized mononuclear unit $W^{VI}(S_2pd)_2$ of all enzymes that have been crystallographically examined (1.85−2.3 Å resolution). The geometry of this unit places additional ligands in a cis arrangement. Structural data together with other considerations and conjectures have led to the putative oxidized active sites **a**−**f** set out in Figure 1.[2,5]

The site in *Pyrococcus furiosus* AOR contains two probable oxygen ligands, neither of which is derived from the protein.[7] Tungsten EXAFS analysis has detected two W═O distances at 1.74 Å.[8] In formaldehyde oxidoreductase from the same organism, an apparent oxygen ligand is

* To whom correspondence should be addressed. E-mail: holm@chemistry.harvard.edu.

(1) Johnson, M. K.; Rees, D. C.; Adams, M. W. W. *Chem. Rev.* **1996**, *96*, 2817−2839.
(2) Hille, R. *Trends Biochem. Sci.* **2002**, *27*, 360−367.
(3) Garner, C. D.; Stewart, L. J. *Met. Ions Biol. Syst.* **2002**, *39*, 699−726.
(4) Roy, R.; Adams, M. W. W. *Met. Ions Biol. Syst.* **2002**, *39*, 673−697.
(5) Vorholt, J. A.; Thauer, R. K. *Met. Ions Biol. Syst.* **2002**, *39*, 571−619.
(6) Abbreviations are given in Chart 1.
(7) Chan, M. K.; Mukund, S.; Kletzin, A.; Adams, M. W. W.; Rees, D. C. *Science* **1995**, *267*, 1463−1469.
(8) George, G. N.; Prince, R. C.; Mukund, S.; Adams, M. W. W. *J. Am. Chem. Soc.* **1992**, *114*, 3521−3523.

10.1021/ic030301k CCC: $27.50
Published on Web 01/30/2004

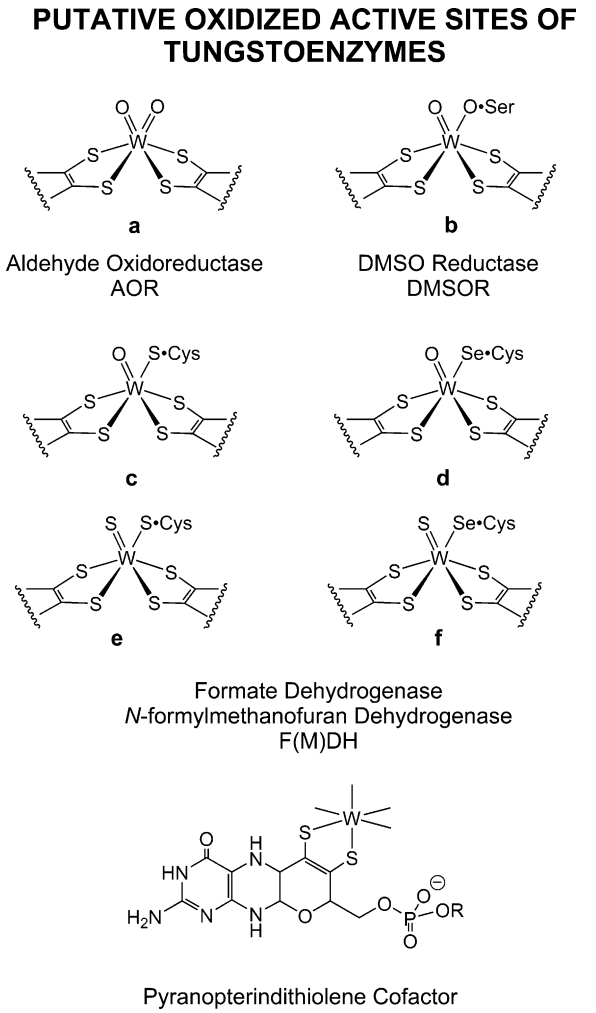

Figure 1. Possible oxidized active sites in tungstoenzymes grouped by family, except for DMSO reductase (see text), and the pyranopterindithiolene cofactor ligand (R absent or a nucleotide).

reported at −2.1 Å.[9] A reasonable proposal is dioxo site **a** or its monoprotonated form $[W^{VI}O(OH)(S_2pd)_2]$, in which case the situation would be analogous to that in molybdenum-containing arsenite oxidase.[10] Site **b** is that of W-DMSOR, an isoenzyme of Mo-DMSOR from *Rhodobacter capsulatus*.[11] While W-DMSOR is not known as a wild-type enzyme and thus is not classified in the foregoing families, it is the only tungstoenzyme for which the complete active site coordination unit is established. Some or all of sites **c**−**f** may apply to members of the F(M)DH family. The only structural information available is for *Desulfovibrio gigas* W-FDH, whose site contains a selenocysteinate and one additional oxygen or sulfur ligand.[12,13] Site **d** is an attractive possibility inasmuch as two *E. coli* Mo-FDH isoenzymes were crystallographically determined to contain the monoprotonated site $[Mo^{VI}(OH)(Se{\cdot}Cys)(S_2pd)_2]$.[14,15]

The sites in Figure 1 are all plausible objectives for synthesis and structural and reactivity examination. Several site analogues have already been prepared. The complexes $[WO_2(bdt)_2]^{2-}$,[16] $[WO_2(ndt)_2]^{2-}$,[17] $[WO_2(mnt)_2]^{2-}$,[18] and $[WO_2(S_2C_2Me_2)_2]^{2-}$ [19] are suitable structural analogues of site **a**. Their reactivity, however, has not been fully investigated in the enzymatic context. The complexes $[WO(OR)(S_2C_2Me_2)_2]^{1-}$ (R = Ph, Pr^i) are excellent structural and reactivity analogues of site **b**. Functional reaction systems based on the reduction of *S*-oxides (DMSOR activity) and *N*-oxides (TMAOR activity) have been amply demonstrated.[20,21] No analogues exist for sites **c**−**f**. The chemistry of bis(dithiolene)tungsten species having been largely unrevealed, we have in recent investigations utilized exploratory synthesis to determine what coordination fragments (equivalently, functional groups) $W^{IV,V}L$ and $W^{VI}LL'$ are capable of existence in bis(dithiolene) species.[19−24] Certain of these then become candidates for functionalities in enzyme sites. Much of this research is summarized elsewhere.[25] We continue that line of inquiry here, directed at unknown functional groups and also, given our interest in FDH, bis(dithiolene)tungsten complexes of formate.

Experimental Section

Preparation of Compounds. All reactions and manipulations were performed under a pure dinitrogen atmosphere using either modified Schlenk techniques or an inert atmosphere box. The following ligand salts were prepared from equimolar reactants and were isolated as colorless crystalline solids from the indicated recrystallization medium: $(Et_4N)(Bu^tCO_2)$, from Bu^tCO_2H and 25% Et_4NOH in methanol, acetonitrile/ether; $(Et_4N)(MeCO_2)$, from Et_4NCl and NaO_2CMe in acetonitrile, acetonitrile/THF/ether; $(Et_4N)(HCO_2)$, from HCO_2Ag and Et_4NCl in methanol. The compound $Me_3SiC_6H_2$-2,4,6-Pr^i_3 was prepared by a procedure similar to that for Me_3SiSPh.[26] Representative compounds were analyzed. All compounds were identified by X-ray structure determinations.

(a) W^{IV} Complexes. $(Et_4N)[W(O_2CMe)(S_2C_2Me_2)_2]$. To a solution of 95.5 mg (0.505 mmol) of $(Et_4N)(MeCO_2)$ in 2 mL of acetonitrile was added a dark purple solution of 226 mg (0.475 mmol) of $[W(CO)_2(S_2C_2Me_2)_2]$[23] in 5 mL of THF. The solution became red-brown immediately with accompanying vigorous gas

(9) Hu, Y.; Faham, S.; Roy, R.; Adams, M. W. W.; Rees, D. C. *J. Mol. Biol.* **1999**, *286*, 899−914.
(10) Ellis, P. J.; Conrads, T.; Hille, R.; Kuhn, P. *Structure* **2001**, *9*, 125−132.
(11) Stewart, L. J.; Bailey, S.; Bennett, B.; Charnock, J. M.; Garner, C. D.; McAlpine, A. S. *J. Mol. Biol.* **2000**, *299*, 593−600.
(12) Raaijmakers, H.; Teixeira, S.; Dias, J. M.; Almendra, M. J.; Brondino, C. D.; Moura, I.; Moura, J. J. G.; Romno, M. J. *J. Biol. Inorg. Chem.* **2001**, *6*, 398−404.
(13) Raaijmakers, H.; Macieira, S.; Dias, J. M.; Texeira, S.; Bursakov, S.; Huber, R.; Moura, J. J. G.; Moura, I.; Romno, M. J. *Structure* **2002**, *10*, 1261−1272.
(14) Boyington, J. C.; Gladyshev, V. N.; Khangulov, S. V.; Stadtman, T. C.; Sun, P. D. *Science* **1997**, *275*, 1305−1308.
(15) Jormakka, M.; Törnroth, S.; Byrne, B.; Iwata, S. *Science* **2002**, *295*, 1863−1868.
(16) Ueyama, N.; Oku, H.; Nakamura, A. *J. Am. Chem. Soc.* **1992**, *114*, 7310−7311.
(17) Oku, H.; Ueyama, N.; Nakamura, A. *Bull. Chem. Soc. Jpn.* **1996**, *69*, 3139−3150.
(18) Das, S. K.; Biswas, D.; Maiti, R.; Sarkar, S. *J. Am. Chem. Soc.* **1996**, *118*, 1387−1397.
(19) Sung, K.-M.; Holm, R. H. *Inorg. Chem.* **2001**, *40*, 4518−4525.
(20) Sung, K.-M.; Holm, R. H. *J. Am. Chem. Soc.* **2001**, *123*, 1931−1943.
(21) Sung, K.-M.; Holm, R. H. *J. Am. Chem. Soc.* **2002**, *124*, 4312−4320.
(22) Lorber, C.; Donahue, J. P.; Goddard, C. A.; Nordlander, E.; Holm, R. H. *J. Am. Chem. Soc.* **1998**, *120*, 8102−8112.
(23) Goddard, C. A.; Holm, R. H. *Inorg. Chem.* **1999**, *38*, 5389−5398.
(24) Sung, K.-M.; Holm, R. H. *Inorg. Chem.* **2000**, *39*, 1275−1281.
(25) Enemark, J. H.; Cooney, J. J. A.; Wang, J.-J.; Holm, R. H. *Chem. Rev.* **2004**, *104*, 1175−1200.
(26) Davis, F. A.; Rizvi, S. Q. A.; Ardecky, R.; Gosciniak, D. J.; Friedman, A. J.; Yocklovich, S. G. *J. Org. Chem.* **1980**, *45*, 1650−1653.

evolution, and was stirred for 35 min. Ether (15 mL) was layered on the reaction mixture. The solid that separated was washed with ether (3 × 2 mL) and dried to afford the product as 189 mg (63%) of a red-brown microcrystalline solid. Absorption spectrum (acetonitrile): λ_{max} (ϵ_M) 330 (4200), 381 (2900), 408 (2900) nm. IR (KBr): ν_{COO} 1439 cm^{-1}. ^{1}H NMR (CD_3CN, anion): δ 1.48 (s, 3), 2.68 (s, 12).

(Et_4N)[$W(O_2CBu^t)(S_2C_2Me_2)_2$]. To a solution of 101 mg (0.437 mmol) of (Et_4N)(Bu^tCO_2) in 1 mL of acetonitrile was added a solution of 201 mg (0.422 mmol) of [$W(CO)_2(S_2C_2Me_2)_2$] in 3 mL of THF. The solution was stirred for 1 h. Ether (25 mL) was layered on the reaction mixture. The solid that separated was washed with ether (3 × 3 mL) and dried to afford the product as 203 mg (74%) of a red-brown microcrystalline solid. Absorption spectrum (acetonitrile): λ_{max} (ϵ_M) 333 (3900), 384 (3300), 403 (3300), 474 (1100), 670 (620) nm. IR (KBr): ν_{COO} 1438 cm^{-1}. ^{1}H NMR (CD_3CN, anion): δ 0.87 (s, 9), 2.68 (s, 12). Anal. Calcd for $C_{21}H_{41}NO_2S_4W$: C, 38.71; H, 6.34; N, 2.15; S, 19.68. Found: C, 38.55; H, 6.41; N, 2.14; S, 19.49.

(Et_4N)[$W(CO)(O_2CH)(S_2C_2Me_2)_2$]. A solution of 21 mg (0.12 mmol) of (Et_4N)(HCO_2) in 0.5 mL of acetonitrile was treated with a solution of 52 mg (0.11 mmol) of [$W(CO)_2(S_2C_2Me_2)_2$] in 1.5 mL of THF at −40 °C. The same color change and gas evolution occurred as in the preceding preparations. The reaction mixture was stirred for 5 min at −40 °C, and cold ether (40 mL) was layered on. The solid that separated was washed with ether (3 × 2 mL) and dried to give the product as 21 mg (32%) of a red microcrystalline solid. ^{1}H NMR (CD_3CN, anion): δ 2.59 (s, 12), 7.95 (s, 1). The compound is unstable in solution at ambient temperature; analytical data could not be obtained.

(Et_4N)[$W(SC_6H_2$-2,4,6-$Pr^i_3)(S_2C_2Me_2)_2$]. A solution of 84 mg (0.13 mmol) of (Et_4N)[$W(O_2CBu^t)(S_2C_2Me_2)_2$] in 1 mL of acetonitrile was treated with 44 mg (0.14 mmol) of $Me_3SiSC_6H_2$-2,4,6-Pr^i_3. The red-brown solution became red immediately. The reaction mixture was stirred for 10 min, and the solvent was removed in vacuo. The residue was washed with ether (3 × 2 mL) and dissolved in 2.5 mL of THF/acetonitrile (4:1 v/v). The solution was filtered through Celite, and ether (40 mL) was layered on the filtrate. The solid which formed was washed with ether (3 × 2 mL) and dried. The product was obtained as 61 mg (60%) of a red microcrystalline solid. Absorption spectrum (acetonitrile): λ_{max} (ϵ_M) 294 (13 600), 313 (sh, 11 700), 345 (sh, 7800), 430 (3500), 517 (1300) nm. ^{1}H NMR (CD_3CN, anion): δ 1.08 (d, 12), 1.17 (d, 6), 2.77 (s, 12), 2.80 (m, 1), 3.72 (m, 2), 6.76 (s, 2). Anal. Calcd for $C_{31}H_{55}NS_5W$: C, 47.44; H, 7.06; N, 1.78; S, 20.43. Found: C, 47.37; H, 6.95; N, 1.74; S, 20.37.

(b) W^{VI} Complexes. (Et_4N)[$WO(O_2CPh)(S_2C_2Me_2)_2$]. Method A. To a suspension of 33 mg (0.058 mmol) of (Et_4N)[$WO(S_2C_2Me_2)_2$][19] in 1 mL of acetonitrile was added a solution of 8.0 mg (0.033 mmol) of dibenzoyl peroxide in 0.5 mL of acetonitrile. The reaction mixture immediately became black and was stirred for 5 min. Cold ether/pentane (25 mL, 1:1 v/v, −40 °C) was layered on the reaction mixture, which was maintained at −40 °C. The solid that separated was washed with ether (3 × 2 mL) and dried to yield the product as 29 mg (73%) of a dark red microcrystalline solid. Absorption spectrum (acetonitrile): λ_{max} (ϵ_M) 381 (sh, 2500), 509 (1300), 610 (1900) nm. IR (KBr): ν_{COO} 1648 cm^{-1}, ν_{WO} 905 cm^{-1}. ^{1}H NMR (CD_3CN, anion): δ 2.26 (s, 12), 7.41 (m, 2), 7.51 (m, 1), 8.01 (m, 2). Anal. Calcd for $C_{23}H_{37}NO_3S_4W$: C 40.17; H, 5.42; N, 2.04; S, 18.65. Found: C, 40.04; H, 5.41; N, 2.06; S, 18.76.

Method B. To a suspension of 41 mg (0.061 mmol) of (Et_4N)[$W(O_2CPh)(S_2C_2Me_2)_2$] in 1 mL of acetonitrile was added a solution of 20 mg (0.060 mmol) of Ph_3AsO in 1 mL of acetonitrile. The black reaction mixture was stirred for 8 min and cooled to −40 °C. Cold ether (20 mL, −40 °C) was layered on, causing separation of 17 mg (41%) of a dark red crystalline solid whose ^{1}H NMR spectrum was identical to the product of method A.

(Et_4N)[$WO(O_2CH)(S_2C_2Me_2)_2$]. To a purple suspension of 30 mg (0.063 mmol) of [$W(CO)_2(S_2C_2Me_2)_2$] in 0.8 mL of Me_2SO was added 12 mg (0.069 mmol) of (Et_4N)(HCO_2). The reaction mixture was stirred for 10 min during which the solid dissolved and a dark red solution developed. Addition of 20 mL of cold ether (0 °C) caused immediate formation of an oily precipitate, which was washed with ether (3 × 3 mL) and dissolved in 3:7 acetonitrile/THF (v/v). The solution was layered with cold ether/pentane (1:1 v/v, −40 °C) and stored at −40 °C. The solid that separated was washed with ether (3 × 2 mL) and dried, giving the product as 11 mg (29%) of a dark red microcrystalline solid. Absorption spectrum (acetonitrile): λ_{max} (ϵ_M) 294 (6300), 358 (2200), 512 (1300), 620 (2000), 687 (1900) nm. IR (KBr): ν_{WO} 887 cm^{-1}, ν_{COO} 1653 cm^{-1}. ^{1}H NMR (CD_3CN, anion): δ 2.23 (s, 12), 8.44 (s, 1).

(Et_4N)[$WO(SC_6H_2$-2,4,6-$Pr^i_3)(S_2C_2Me_2)_2$]. To a solution of 62 mg (0.079 mmol) of (Et_4N)[$W(SC_6H_2$-2,4,6-$Pr^i_3)(S_2C_2Me_2)_2$] in 1 mL of acetonitrile/THF (1:4 v/v) was added a solution of 27 mg (0.081 mmol) of Ph_3AsO in 1 mL of THF. The red solution immediately changed to purple. The reaction mixture was stirred for 5 min, cold ether (20 mL, −40 °C) was layered on, and the mixture was maintained at −40 °C. The solid that separated was washed with cold ether (3 × 2 mL) and dried. The product was obtained as 43 mg (68%) of a purple microcrystalline solid. Absorption spectrum (acetonitrile): λ_{max} (ϵ_M) 340 (5100), 411 (3600), 556 (3800) nm. IR (KBr): ν_{WO} 902 cm^{-1}. ^{1}H NMR (CD_3CN, anion): δ 1.19 (d, 12), 1.22 (d, 6), 2.23 (s, 12), 2.86 (m, 1), 4.23 (m, 2), 6.97 (s, 2). Anal. Calcd for $C_{31}H_{55}NOS_5W$: C, 46.49; H, 6.92; N, 1.75; S, 20.02. Found: C, 46.58; H, 7.03; N, 1.79; S, 20.08.

(Et_4N)[$WS(SC_6H_2$-2,4,6-$Pr^i_3)(S_2C_2Me_2)_2$]. A solution of 62 mg (0.079 mmol) of (Et_4N)[$W(SC_6H_2$-2,4,6-$Pr^i_3)(S_2C_2Me_2)_2$] in 1 mL of acetonitrile/THF (1:4 v/v) was treated with a solution of 22 mg (0.079 mmol) of $(PhCH_2S)_2S$ in 1 mL of THF. The red solution turned to red-purple immediately. The reaction mixture was stirred for 5 min, and cold ether (20 mL, −40 °C) was layered on. The mixture was maintained at −40 °C. The solid that separated was washed with ether (3 × 2 mL) and dried. The product was obtained as 27 mg (42%) of a red microcrytalline solid. Absorption spectrum (acetonitrile): λ_{max} (ϵ_M) 274 (9700), 335 (6500), 391 (5200), 524 (4100) nm. ^{1}H NMR (CD_3CN, anion): δ 1.19 (d, 12), 1.24 (d, 6), 2.32 (s, 12), 2.87 (m, 1), 4.17 (m, 2), 6.92 (s, 2). Anal. Calcd for $C_{31}H_{55}NS_6W$: C 45.52; H, 6.78; N, 1.71; S, 23.52. Found: C, 45.46; H, 6.84; N, 1.68; S, 23.14.

(Et_4N)[$WOCl(S_2C_2Me_2)_2$]. A red solution of 30 mg (0.042 mmol) of (Et_4N)$_2$[$WO_2(S_2C_2Me_2)_2$][19] in 0.8 mL of acetonitrile was treated with 10 mg (0.092 mmol) of Me_3SiCl. The reaction mixture immediately assumed a purple color and was stirred for 5 min. Solvent was removed in vacuo, and the residue was extracted with 4 mL of acetonitrile/THF (1:4 v/v). Cold ether (20 mL, −40 °C) was layered onto the extract, and the mixture was maintained at −40 °C for 2 days. The solid was collected, washed with ether (3 × 2 mL), and dried to afford the product as 8.0 mg (29%) of purple-black microcrystalline solid. ^{1}H NMR (CD_3CN, anion): δ 2.26 (s).

In the sections which follow, tungsten complexes are referred to by the numerical designations in Chart 1.

X-ray Structure Determinations. The nine compounds in Table 1 were structurally identified. Suitable crystals of (Et_4N)[**2**, **4**] (red-brown plates), (Et_4N)[**3**, **5**] (red-brown blocks), (Et_4N)[**6**, **7**, **10**] (dark purple blocks), and (Et_4N)[**8**, **9**] (thin purple plates) were

Table 1. Crystallographic Data[a] for Bis(dithiolene)W(IV,VI) Complexes

	(Et$_4$N)[**2**]	(Et$_4$N)[**3**]	(Et$_4$N)[**4**]	(Et$_4$N)[**5**]	(Et$_4$N)[**6**]	(Et$_4$N)[**7**]	(Et$_4$N)[**8**]	(Et$_4$N)[**9**]	(Et$_4$N)[**10**]
formula	$C_{18}H_{35}NO_2S_4W$	$C_{21}H_{41}NO_2S_4W$	$C_{18}H_{33}NO_3S_4W$	$C_{31}H_{55}NS_5W$	$C_{23}H_{37}NO_3S_4W$	$C_{17}H_{33}NO_3S_4W$	$C_{31}H_{55}NOS_5W$	$C_{31}H_{55}NOS_6W$	$C_{16}ClH_{32}NOS_4W$
fw	609.56	651.64	623.54	785.91	687.63	611.53	801.91	817.98	601.97
cryst syst	monoclinic	orthorhombic	monoclinic	monoclinic	monoclinic	monoclinic	monoclinic	monoclinic	monoclinic
space group	*C*2	*Pnma*	$P2_1/n$	$P2_1/n$	$P2_1/c$	$P2_1/c$	$P2_1/c$	$P2_1/c$	$P2_1/n$
T, K	213	213	193	193	193	193	193	193	213
Z	2	4	4	4	4	4	4	4	4
a, Å	15.725(3)	17.734(1)	10.009(7)	11.397(2)	14.183(2)	8.974(1)	10.71(1)	20.84(3)	8.960(1)
b, Å	7.949(2)	16.533(1)	18.64(1)	11.463(2)	11.792(2)	15.043(2)	18.05(2)	10.91(2)	16.507(2)
c, Å	9.710(2)	9.4002(7)	13.668(9)	19.149(2)	17.008(2)	17.928(3)	18.79(2)	16.38(3)	15.718(2)
β, deg	97.093(4)		108.99(2)	109.853(2)	97.735(2)	97.576(3)	93.86(2)	93.73(2)	91.828(2)
V, Å^3	1204.4(4)	2756.1(4)	2411(3)	3591.7(7)	2818.7(6)	2399.1(6)	3625(6)	3713(10)	2323.6(4)
d_{calcd}, g/cm^3	1.681	1.570	1.718	1.453	1.620	1.693	1.468	1.454	1.721
μ, mm^{-1}	5.154	4.509	5.516	3.527	4.418	5.179	3.498	3.469	5.450
θ range, deg	2.11−22.50	2.30−22.50	1.92−22.50	1.37−22.50	2.11−22.50	1.77−25.00	1.57−22.50	2.11−22.50	1.79−28.32
GOF (F^2)	1.152	1.1561	1.096	0.958	1.013	0.854	0.885	0.643	1.019
R_1[b] (wR_2[c]), %	2.91(7.22)	2.67(7.61)	3.56(9.56)	2.28(5.09)	2.32(5.80)	2.41/4.38	3.71(7.78)	6.58(13.61)	7.80(14.27)

[a] Mo Kα radiation. [b] $R_1 = \sum||F_o| - |F_c||/\sum|F_o|$. [c] $wR_2 = \{\sum[w(F_o^2 - F_c^2)^2]/\sum[w(F_o^2)^2]\}^{1/2}$.

Chart 1. Designation of Complexes and Abbreviations

$[W^{IV}(O_2CPh)(S_2C_2Me_2)_2]^{1-}$	**1**[19]
$[W^{IV}(O_2CMe)(S_2C_2Me_2)_2]^{1-}$	**2**
$[W^{IV}(O_2CBu^t)(S_2C_2Me_2)_2]^{1-}$	**3**
$[W^{IV}(CO)(O_2CH)(S_2C_2Me_2)_2]^{1-}$	**4**
$[W^{IV}(SC_6H_2\text{-}2,4,6\text{-}Pr^i_3)(S_2C_2Me_2)_2]^{1-}$	**5**
$[W^{VI}O(O_2CPh)(S_2C_2Me_2)_2]^{1-}$	**6**
$[W^{VI}O(O_2CH)(S_2C_2Me_2)_2]^{1-}$	**7**
$[W^{VI}O(SC_6H_2\text{-}2,4,6\text{-}Pr^i_3)(S_2C_2Me_2)_2]^{1-}$	**8**
$[W^{VI}S(SC_6H_2\text{-}2,4,6\text{-}Pr^i_3)(S_2C_2Me_2)_2]^{1-}$	**9**
$[W^{VI}OCl(S_2C_2Me_2)_2]^{1-}$	**10**

AOR, aldehyde oxidoreductase; bdt, benzene-1,2-dithiolate(2-); DMSOR, dimethylsulfoxide reductase; F(M)DH, formate (*N*-formylmethanofuran) dehydrogenase; mnt, maleonitriledithiolate(2-); ndt, naphthalene-2,3-dithiolate(2-), S_2pd, pyranopterindithiolene(2-); TMAOR, trimethylamine *N*-oxide reductase

obtained either by layering ether onto or ether vapor diffusion into acetonitrile solutions. These mixtures were allowed to stand 2−3 days at room temperature ((Et$_4$N)[**2**, **3**, **5**]) or at −40 °C (others). Crystals were coated in grease and mounted on a Siemens (Bruker) SMART CCD area detector instrument with Mo Kα radiation. Data were collected at 213 or 193 K with ω scans of 0.3° per frame, with 10, 20, or 30 s frames, such that 1271 frames were collected for a hemisphere of data.

The first 50 frames were recollected at the end of the data collection to monitor intensity decay; no significant decay was observed for any compound. Data out to 2θ of 50° and 56° were used for (Et$_4$N)[**7**] and (Et$_4$N)[**10**], respectively, but for the other compounds data out to 2θ of 45° were employed because of the low quality of the high-angle data. Cell parameters were retrieved using SMART software and refined using SAINT software on all observed reflections between 2θ of 3° and the upper thresholds. Data reduction was performed with SAINT, which corrects for Lorentz polarization and decay. Absorption corrections were applied with SADABS, as described by Blessing.[27] All space groups were assigned by analysis of symmetry and systematic absences determined by XPREP. The space group for (Et$_4$N)[**2**] was selected from noncentrosymmetric choices of the basis of the lowest combined figure of merit. Structures were solved by direct methods with SHELXL-97 and refined against all data in the 2θ ranges by full-matrix least-squares on F^2 using SHELXL-97. All non-hydrogen atoms, including those of disordered cations, were refined anisotropically. Hydrogen atoms at idealized positions were included in final refinements. Cell parameters and final agreement factors are given in Table 1. (See paragraph at the end of this article for Supporting Information available.)

Other Physical Measurements. All measurements were performed under anaerobic conditions. Absorption spectra were recorded with a Varian Cary 50 Bio spectrophotometer. ^{1}H NMR spectra were obtained with Varian Mercury 300/400 spectrometers. IR spectra were measured in KBr pellets with a Nicolet 5PC FT-IR instrument.

Results and Discussion

We seek molecules that are analogous to the putative bis(dithiolene)tungsten sites **c**−**f** in Figure 1 and examples of formate binding to tungsten centers that are possibly pertinent to one or more reaction stages of FDH. The synthetic scheme is set out in Figure 2. As in previous synthetic studies,[19−21,23,24] we utilize $[W(CO)_2(S_2C_2Me_2)_2]$,[23,28] whose carbonyl groups are labile to substitution, as a starting material. Isolated yields are indicated below. All new complexes were characterized by X-ray structure determinations; structures are shown in Figures 3−6, and leading structural parameters are collected in Tables 2 and 3. For the most part, these parameters are in good agreement with closely related molybdenum[29,30] and tungsten[19,20,23,24] bis(dithiolenes), and do not require further discussion. The ranges of mean C−C and S−C bond distances are 1.33−1.34 Å and 1.73−1.79 Å, respectively. These values are sufficiently close to the typical bond lengths $(sp^2)C{=}C(sp^2) = 1.331(9)$ Å and $S{-}C(sp^2) = 1.75(2)$ Å[31] to warrant description of the ligand as a classical ene-1,2-dithiolate, as is the case for all bis(dithiolene)tungsten

(27) Blessing, R. H. *Acta Crystallogr.* **1995**, *A51*, 33−38.

(28) Fomitchev, D.; Lim, B. S.; Holm, R. H. *Inorg. Chem.* **2001**, *40*, 645−654.

(29) Lim, B. S.; Donahue, J. P.; Holm, R. H. *Inorg. Chem.* **2000**, *39*, 263−273.

(30) Lim, B. S.; Holm, R. H. *J. Am. Chem. Soc.* **2001**, *123*, 1920−1930.

(31) Allen, F. H.; Kennard, O.; Watson, D. G.; Brammer, L.; Orpen, A. G.; Taylor, R. In *International Tables of Crystallography*; Wilson, A. J. C., Ed.; Kluwer Academic Publishers: Boston, 1995; section 9.5.

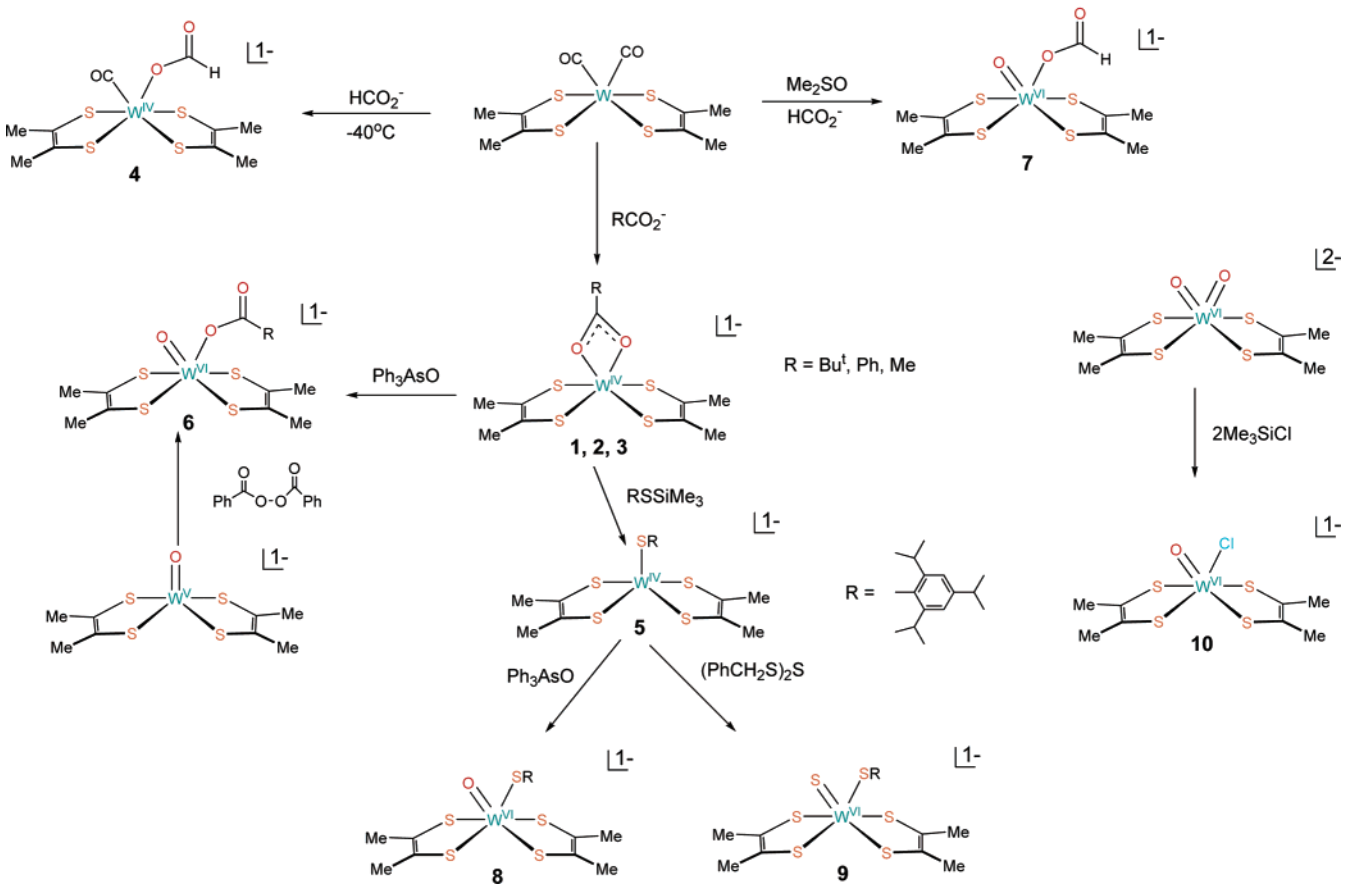

Figure 2. Synthetic scheme for bis(dithiolene)tungsten complexes based on $[W(CO)_2(S_2C_2Me_2)_2]$ and affording W^{IV} (**1**−**5**) and W^{VI} (**6**−**10**) complexes.

Table 2. Selected Bond Distances (Å) and Angles (deg) of Bis(dithiolene)W(IV) Complexes

	2	**3**	**4**	**5**
W−S[a]	2.328(6)	2.301(1)	2.37(2)	2.313(5)
W−S_{ax}[b]				2.319(1)
W−O[a]	2.178(6)	2.167(3)	2.132(7)	
W−C			2.018(9)	
S−C[a]	1.77(1)	1.75(2)	1.744(9)	1.79(1)
C−C[a]	1.34(2)	1.33(1)	1.334(1)	1.325(1)
δ[c]	0.799	0.805	0.784	0.696
θ_d[d]	126.0	124.7	128.1	132.7

[a] Mean values with standard deviation from the mean. [b] Axial ligand. [c] Perpendicular displacement of W atom from S_4 least-squares plane. [d] Dihedral angle between WS_2 planes.

Table 3. Selected Bond Distances (Å) and Angles (deg) of Bis(dithiolene)W(VI) Complexes

	6	**7**	**8**	**9**	**10**
W−S[a,b]	2.406(5)	2.392(7)	2.39(2)	2.374(8)	2.381(9)
W−S_{trans}[c]	2.445(1)	2.420(1)	2.499(3)	2.436(7)	2.465(4)
W═O/S	1.721(3)	1.717(3)	1.749(6)	2.120(7)	1.824(8)
W−O/S/Cl	2.066(3)	2.087(3)	2.436(3)	2.447(8)	2.402(4)
S−C[a]	1.75(1)	1.75(1)	1.74(2)	1.75(2)	1.73(4)
C−C[a]	1.34(1)	1.33(2)	1.34(2)	1.34(1)	1.33(3)
O/S−W−S_{trans}	143.5(1)	138.7(1)	153.4(2)	153.0(3)	149.0(3)
O/S−W−O/S/Cl	94.0(1)	88.7(1)	91.4(2)	96.4(2)	91.5(3)
S−W−S[d]	153.3(4)	151.8(1)	158.5(1)	156.1(2)	156.9(2)
θ_d[e]	103.0	108.0	96.9	94.4	84.2(1)

[a] Mean values with standard deviation from the mean. [b] Mean of 3. [c] Trans to oxo or sulfido. [d] Transoid angle. [e] Dihedral angle between WS_2 chelate planes.

complexes previously prepared. Consequently, the oxidation state designations $W^{IV,VI}$ are appropriate (Chart, Figure 2).

Formate and Other Carboxylate Complexes. Reaction of the dicarbonyl with 1 equiv of formate in reaction 1 at low temperature affords the monocarbonyl formate complex **4** (32%). This species is prone to decomposition at room temperature. In a second experiment, the dicarbonyl was treated with 1 equiv of formate in Me_2SO, presumably generating **4**. Thereafter, oxo transfer reaction 2 ensues, affording the $W^{VI}O$ complex **7** (29%) in reaction 2 which is analogous to the reduction of *N*- and *S*-oxides with $[W(OR)(S_2C_2Me_2)_2]^{1-}$.[20,21] The structures of the two complexes (Figure 3) reveal different shapes. Complex **4** shows

$$[W(CO)_2(S_2C_2Me_2)_2] + HCO_2^- \rightarrow [W(CO)(HCO_2)(S_2C_2Me_2)_2]^{1-} + CO \quad (1)$$

$$[W(CO)(HCO_2)(S_2C_2Me_2)_2]^{1-} + Me_2SO \rightarrow [WO(HCO_2)(S_2C_2Me_2)_2]^{1-} + CO + Me_2S \quad (2)$$

a dihedral angle $\theta_d = 128.1°$ (Table 2) which approaches that (120°) for idealized trigonal prismatic (C_{2v}) geometry.

Very similar values are found for the monocarbonyls $[M^{IV}(CO)L(S_2C_2Me_2)_2]^{1-}$ (M = Mo,[29] W[24]). Complex **7** has $\theta_d = 108.0°$ and an S−W−S transoid angle of 151.8°

$[W^{IV}(CO)(HCO_2)(S_2C_2Me_2)_2]^{1-}$

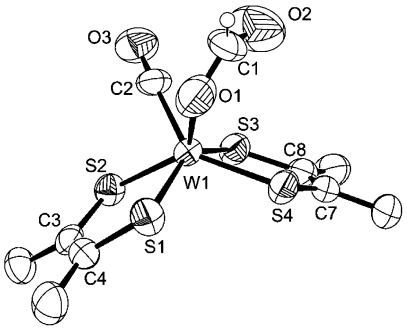

$[W^{VI}O(HCO_2)(S_2C_2Me_2)_2]^{1-}$

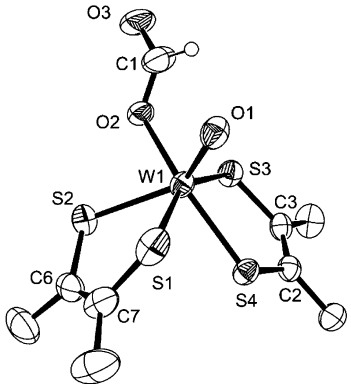

Figure 3. Structures of $[W(CO)(HCO_2)(S_2C_2Me_2)_2]^{1-}$ (**4**, upper) and $[WO(HCO_2)(S_2C_2Me_2)_2]^{1-}$ (**7**, lower). In this and succeeding figures, 50% probability ellipsoids and partial atom labeling schemes are shown.

(involving sulfur atoms of different chelate rings). For an octahedron, $\theta_d = 90°$ and the transoid angle is 180° (136° for a trigonal prism). Consequently, oxo transfer product **7** possesses a distorted octahedral stereochemistry similar to that observed for complexes such as $[WO(OPh)(S_2C_2Me_2)_2]^{1-}$ ($\theta_d = 99.8°$, transoid angle 153.5°).[20] A sufficient body of information now exists to demonstrate the generality of the structural changes in oxo transfer reaction 3 of bis(dithiolene) complexes with M = Mo and W, including those reported here (compare the W^{IV} and $W^{VI}O$ structures in Figures 3−5). With square pyramidal M^{IV}, this is the presumed intrinsic change in proteins, a matter supported by the structural correspondence between $[WO(OPh)(S_2C_2Me_2)_2]^{1-}$ and the oxidized site in the W-DMSOR isoenzyme from *Rhodobacter capsulatus*.[20]

$$[M^{IV}L(S_2C_2R_2)_2]^{1-}\ (\text{sq pyramidal}),$$
$$[M^{IV}LL'(S_2C_2R_2)_2]^{1-}\ (\text{trigonal prismatic}) + XO \rightarrow$$
$$[M^{VI}OL(S_2C_2R_2)_2]^{1-}\ (\text{distorted oct}) + X \quad (3)$$

Formate complexes of tungsten are uncommon and are primarily confined to low-valent mononuclear species with η^1 coordination.[32−34] Recently, $[M^{IV}{}_3O_4]^{4+}$ and $[M^{IV}{}_3S_4]^{4+}$ clusters (M = Mo, W) have been shown to bind formate as η^1 terminal ligands.[35] Examples exist with other elements

(32) Kundel, P.; Berke, H. *J. Organomet.Chem.* **1986**, *314*, C31−C33.
(33) Tso, C. C.; Cutler, A. R. *Inorg. Chem.* **1990**, *29*, 471−475.

$[W^{IV}(MeCO_2)(S_2C_2Me_2)_2]^{1-}$

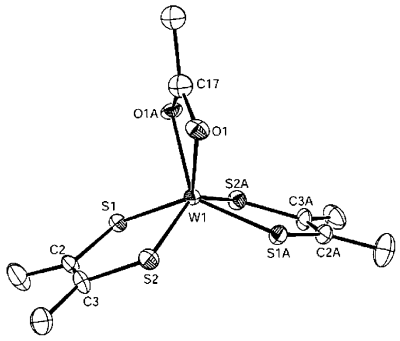

$[W^{VI}O(PhCO_2)(S_2C_2Me_2)_2]^{1-}$

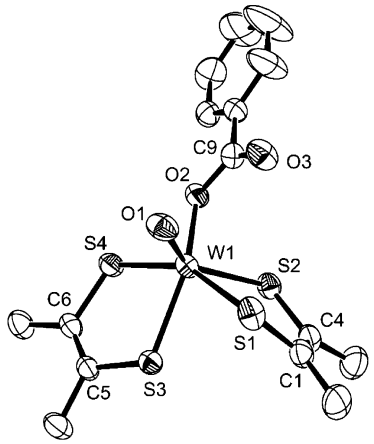

Figure 4. Structures of $[W(MeCO_2)(S_2C_2Me_2)_2]^{1-}$ (**2**, upper) and $[WO(PhCO_2)(S_2C_2Me_2)_2]^{1-}$ (**6**, lower). In the acetate structure, atoms *n* and *n*A are related by a crystallographically imposed 2-fold axis.

of both η^1 and η^2 interactions.[36] Complexes **4** and **7** are the first structurally proven examples of formate binding to mononuclear W^{IV} or W^{VI}. They presumably simulate η^1 substrate binding, should this occur in enzymes, but the complexes lack the selenocysteinate ligand present in the active site of *D. gigas* W-FDH.

Carboxylate complexes **1**[19], **2** (63%), and **3** (74%) are readily prepared by displacement of both carbonyl groups in reaction 4. The carboxylate groups exhibit essentially symmetric η^2 coordination such that the molecules approach C_{2v} symmetry (Figures 4 and 6). In acetate complex **2**, an imposed 2-fold axis bisects the carboxylate chelate ring. Benzoate complex **1** undergoes oxo transfer with Ph_3AsO to afford **6** (41%). The complex may be obtained more efficiently (73%) by reaction 5 in which W^V reduces dibenzoyl peroxide to benzoate, which is captured as an η^1 ligand by W^{VI}. Complexes **6** and **7** have the same distorted octahedral structure and are nearly isometric (Table 3).

$$[W(CO)_2(S_2C_2Me_2)_2] + RCO_2^- \rightarrow$$
$$[W(O_2CR)(S_2C_2Me_2)_2]^{1-} + 2CO \quad (4)$$
$$[WO(S_2C_2Me_2)_2]^{1-} + PhC(O)OOC(O)Ph \rightarrow$$
$$[WO(O_2CPh)(S_2C_2Me_2)_2]^{1-} + PhCO_2^{\bullet} \quad (5)$$

$[W^{IV}(SC_6H_2\text{-}2,4,6\text{-}Pr^i_3)(S_2C_2Me_2)_2]^{1-}$

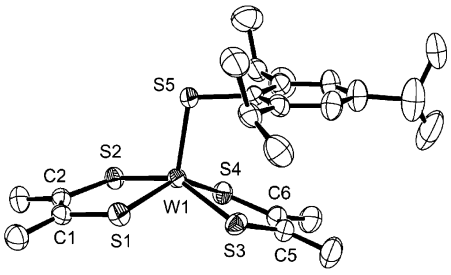

$[W^{VI}O(SC_6H_2\text{-}2,4,6\text{-}Pr^i_3)(S_2C_2Me_2)_2]^{1-}$

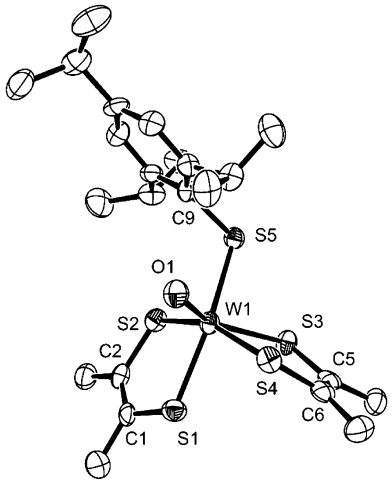

Figure 5. Structures of $[W(SC_6H_2\text{-}2,4,6\text{-}Pr^i_3)(S_2C_2Me_2)_2]^{1-}$ (**5**, upper) and $[WO(SC_6H_2\text{-}2,4,6\text{-}Pr^i_3)(S_2C_2Me_2)_2]^{1-}$ (**8**, lower).

Thiolate Complexes. The most obvious route to analogues of the five-coordinate reduced enzyme sites $[M^{IV}(S/Se\text{·}Cys)(S_2\text{-}pd)_2]$ is by displacement of both carbonyls in $[M(CO)_2(S_2C_2\text{-}Me_2)_2]$. Such species are potentially subject to oxo or sulfido atom transfer, affording analogues of **c**−**f** (Figure 1). The displacement route has been previously investigated in detail for M = Mo[29,30] and W.[19,24] The complexes $[Mo(QR)\text{-}(S_2C_2Me_2)_2]^{1-}$ (Q = S, Se) are accessible by displacement with extremely bulky thiolates (R = 2-adamantyl). Less hindered thiolates and selenolates form the monocarbonyl products $[Mo(CO)(QR)(S_2C_2Me_2)_2]^{1-}$. However, with tungsten the same thiolates and selenolates, including the 2-adamantyl derivatives, afford only the monocarbonyls $[W(CO)(QR)(S_2C_2Me_2)_2]^{1-}$. Attempts at decarbonylation have not been successful. The relative stabilities of the molybdenum and tungsten monocarbonyls are discussed elsewhere.[24]

Reaction 6 provides the first route to complexes of the type $[W(SR)(S_2C_2Me_2)_2]^{1-}$, and utilizes the enthalpic change in forming a Si−O versus a Si−S bond. Treatment of **3** with 1 equiv of the hindered silylthiolate affords complex **5** (60%) as a red microcrystalline solid. While the matter has not been exhaustively explored, less hindered reactants (including $Me_3\text{-}SiSPh$) do not yield tractable products. Complex **5** (Figure 5, Table 2) is isostructural with $[Mo(SC_6H_2\text{-}2,4,6\text{-}Pr^i_3)(S_2C_2\text{-}Me_2)_2]^{1-}$ (Mo−S_{ax} = 2.31 Å, δ = 0.706 Å, θ_d = 132.1°), which is accessible by a carbonyl displacement reaction.[29]

$$[W(O_2CBu^t)(S_2C_2Me_2)_2]^{1-} + Me_3SiSC_6H_2\text{-}2,4,6\text{-}Pr^i_3 \rightarrow [W(SC_6H_2\text{-}2,4,6\text{-}Pr^i_3)(S_2C_2Me_2)_2]^{1-} + Me_3SiOCOBu^t \quad (6)$$

The near-identity of the structural parameters indicates that the inability to displace both carbonyls from $[W(CO)_2(S_2C_2\text{-}Me_2)_2]$ versus $[Mo(CO)_2(S_2C_2Me_2)_2]$ is not steric in origin but in intrinsically stronger carbonyl binding in the tungsten complex.

The availability of complex **5** has permitted the investigation of atom transfer reactions. Oxo transfer reaction 7 leads to the purple $W^{VI}O$ species **8** (68%) while sulfur transfer reaction 8 affords the red $W^{VI}S$ complex **9** (42%), whose

$[W^{IV}(Bu^tCO_2)(S_2C_2Me_2)_2]^{1-}$

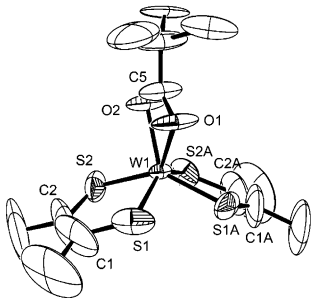

$[W^{VI}S(SC_6H_2\text{-}2,4,6\text{-}Pr^i_3)(S_2C_2Me_2)_2]^{1-}$

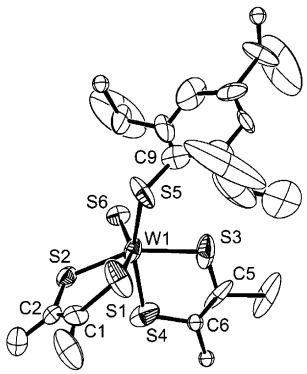

$[W^{VI}OCl(S_2C_2Me_2)_2]^{1-}$

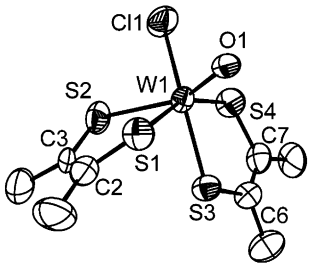

Figure 6. Structures of $[W(Bu^tCO_2)(S_2C_2Me_2)_2]^{1-}$ (**3**, upper), $[WS(SC_6H_2\text{-}2,4,6\text{-}Pr^i_3)(S_2C_2Me_2)_2]^{1-}$ (**9**, middle), and $[WOCl(S_2C_2Me_2)_2]^{1-}$ (**10**, lower).

(34) Baur, J.; Jacobsen, H.; Burger, P.; Artus, G.; Berke, H.; Dahlenberg, L. *Eur. J. Inorg. Chem.* **2000**, 1411−1422.
(35) Brorson, M.; Hazell, A.; Jacobsen, C. J. H.; Schmidt, I.; Villadsen, J. *Inorg. Chem.* **2000**, *39*, 1346−1350.
(36) Gibson, D. H. *Coord. Chem. Rev.* **1999**, *185*−*186*, 335−355.

Table 4. Functional Groups in Bis(dithiolene)W(IV, V, VI) Complexes

ox. state	group	refs[d]
W(VI)	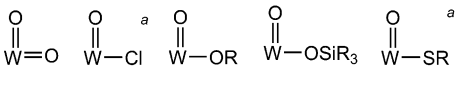	16-19,22; 22,a; 20,37; 22; a
	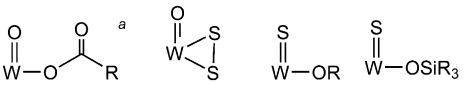	a; 18; 19; 22
		a
W(V)	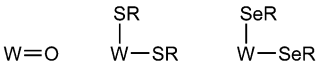	16,19,22,23,38; 19; 19
W(IV)	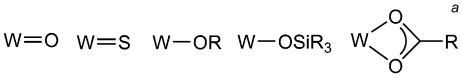	16,22,23,38; 19,23; 20,21,24,37; 22; 19,a
	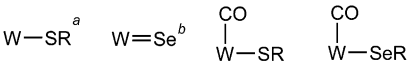	a; 23; 19,24; 19,24
	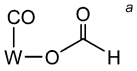	a
W(?)[c]	$W(CO)_2$ $W(CNR)_2$ $W(P(OR)_3)_2$	23,28; 23; 23

[a] This work. [b] Not proven by a structure determination. [c] Ambiguous oxidation state. [d] References to a given group delimited by a semicolon.

stability to isolation is noteworthy given the strongly reducing ligand environment. Reaction 7 is the first example of oxo transfer of a dithiolene molybdenum or tungsten complex with an axial thiolate ligand.

$$[W(SC_6H_2\text{-}2,4,6\text{-}Pr^i_3)(S_2C_2Me_2)_2]^{1-} + Ph_3AsO \rightarrow [WO(SC_6H_2\text{-}2,4,6\text{-}Pr^i_3)(S_2C_2Me_2)_2]^{1-} + Ph_3As \quad (7)$$

$$[W(SC_6H_2\text{-}2,4,6\text{-}Pr^i_3)(S_2C_2Me_2)_2]^{1-} + (PhCH_2S)_2S \rightarrow [WS(SC_6H_2\text{-}2,4,6\text{-}Pr^i_3)(S_2C_2Me_2)_2]^{1-} + (PhCH_2S)_2 \quad (8)$$

Reaction 8 is precedented only by the formation of $[WS(OSiR_3)(bdt)_2]^{1-}$ from $[W(OSiR_3)(bdt)_2]^{1-}$ and dibenzyltrisulfide.[22] Complexes **8** and **9** are essentially isostructural (Figures 5 and 6, Table 3) with distorted octahedral stereochemistry and exert a substantial trans influence of ca. 0.07−0.10 Å on the bond length of an opposite chelate ring sulfur atom.

Extensive attempts were made to prepare the W^{IV} complexes $[W(SeR)(S_2C_2Me_2)_2]^{1-}$, related to **5** and $[Mo(Se\text{-}2\text{-}adamantyl)(S_2C_2Me_2)_2]^{1-}$.[30] Among the reactions investigated were those analogous to 6 with different Me_3SiSeR reagents, including R = 2,4,6-$C_6H_2R'_3$ (R′ = Pr^i, Bu^t, Ph) at room temperature and −40 °C. While ^1H NMR spectra indicated a slight amount of product formation, no tractable materials were isolated. Silylation of $[WO_2(S_2C_2Me_2)_2]^{2-}$ resulted in the synthesis of chloride complex **10** (Figure 1) with a distorted octahedral structure (Figure 6, Table 3). This complex is analogous to $[WOCl(bdt)_2]^{1-}$, which undergoes chloride substitution by benzenethiolate.[22] Reaction systems based on **10** and selenolates also failed to produce stable products. The inability to isolate the selenolate counterparts of thiolate complex **5** is unexpected and, at present, not readily explained.

Tungsten Functional Groups. The completion of the scheme of Figure 2 provides an expanded array of functional groups in bis(dithiolene)tungsten(IV,V,VI) complexes. The currently available set of these groups is summarized in Table 4,[37,38] which supplants several earlier versions.[19,25] Previously unknown groups include $W^{VI}O(SR)$ (**c**), $W^{VI}S(SR)$ (**e**), $W^{VI}O(O_2CR)$, (R = H, Ph), $W^{IV}SR$, and $W^{IV}(CO)(O_2CH)$. Additional examples of $W^{IV}(O_2CR)$ and $W^{VI}OCl$ have been prepared. There are now analogue complexes for all sites in Figure 1 except the two involving selenocysteinate ligation (**d**, **f**). The biological relevance of these molecules as structural and functional analogues requires a more complete specificiation of enzyme sites. In the meantime, we note the relation to defined molybdoenzyme sites and the possibility of corresponding reactivity. The $W^{VI}O(OR)/W^{IV}(OR)$ complexes are meaningful reactivity analogues of DMSOR and TMAOR enzymes and of tungsten isoenzymes,[20,21] and may appertain to selenate reductase.[39] The pair $W^{VI}O_2/W^{IV}O$ is

(37) Lim, B. S.; Sung, K.-M.; Holm, R. H. *J. Am. Chem. Soc.* **2000**, *122*, 7410−7411.
(38) Davies, E. S.; Aston, G. M.; Beddoes, R. L.; Collison, D.; Dinsmore, A.; Docrat, A.; Joule, J. A.; Wilson, C. R.; Garner, C. D. *J. Chem. Soc., Dalton Trans.* **1998**, 3647−3656.

related to the active sites of arsenite oxidase, which has two pyranopterindithiolene ligands and no polypeptide ligand,[10,40] and possibly to assimilatory nitrate reductases[41,42] and AOR (vide supra) which apparently share these properties. The pair $W^{VI}O(SR)/W^{IV}(SR)$ is related to the sites of a dissimilatory nitrate reductase, which features cysteinate ligation.[43] As noted, FDH analogue sites are currently missing. The substitution of Cys·S for Cys·Se in *E. coli* FDH_H results in a ~300-fold decrease in k_{cat},[44] implying a direct role of the selenocysteinate residue in catalysis. Possibly the preceding pair of complexes may be useful in determining whether formate can be bound and oxidized in the absence of selenolate ligation. While there is as yet no evidence for carboxylate ligation in tungstoenzymes, unsymmetrical $Mo(O_2C_{Asp})$ coordination has been found in a nitrate reductase of *E. coli*.[45] Our present research investigates certain complexes in Table 4 as atom transfer reactants in the transformation of biological substrates of molybdo- and tungstoenzymes.

Acknowledgment. This research was supported by NSF Grant CHE 0237419. We thank D. V. Partyka for the synthesis and structure of complex **10**.

Supporting Information Available: X-ray crystallographic files in CIF format for the structure determinations of the nine compounds in Table 1. This material is available free of charge via the Internet at http://pubs.acs.org.

IC030301K

(39) Maher, M. J.; Macy, J. M. *Acta Crystallogr.* **2002**, *D58*, 706−708.
(40) Conrads, T.; Hemann, C.; George, G. N.; Pickering, I. J.; Prince, R. C.; Hille, R. *J. Am. Chem. Soc.* **2002**, *124*, 11276−11277.
(41) Dias, J. M.; Than, M. E.; Humm, A.; Huber, R.; Bourenkov, G. P.; Bartunik, H. D.; Bursakov, S.; Calvete, J.; Caldeira, J.; Carneiro, C.; Moura, J. J. G.; Moura, I.; Romno, M. J. *Structure* **1999**, *7*, 65−79.
(42) Axley, M. J.; Böck, A.; Stadtman, T. C. *Proc. Natl. Acad. Sci. U.S.A.* **1991**, *88*, 8450−8454.
(43) Dias, J. M.; Than, M. E.; Humm, A.; Huber, R.; Bourenko, G. P.; Bartunik, H. D.; Bursakov, S.; Calvete, J.; Carneiro, C.; Moura, J. J. G.; Moura, I.; Romno, M. J. *Structure* **1999**, *7*, 65−79.
(44) Axley, M. J.; Böck, A.; Stadtman, T. C. *Proc. Natl. Acad. Sci. U.S.A.* **1991**, *88*, 8450−8454.
(45) Bertero, M. G.; Rothery, R. A.; Palak, M.; Hou, C.; Lim, D.; Blasco, F.; Weiner, J. H.; Strynadka, N. J. C. *Nat. Struct. Biol.* **2003**, *10*, 681−687.